Conserved secondary structure in the actinorhodin polyketide synthase acyl carrier protein from *Streptomyces coelicolor* A3(2) and the fatty acid synthase acyl carrier protein from *Escherichia coli*

Matthew P. Crump[a], John Crosby[a], Christopher E. Dempsey[b], Martin Murray[a],
David A. Hopwood[c], Thomas J. Simpson[a],*

[a]*School of Chemistry (University of Bristol Molecular Recognition Centre), Bristol University, Cantock's Close, Bristol BS8 1TS, UK*
[b]*Department of Biochemistry (University of Bristol Molecular Recognition Centre), Bristol University, University Walk, Bristol BS8 1TD, UK*
[c]*John Innes Centre, Norwich NR4 7UH, UK*

Abstract **The acyl carrier protein (ACP) of *Streptomyces coelicolor* A3(2) functions as a molecular chaperone during the biosynthesis of the polyketide actinorhodin (*act*). Here we compare structural features of the polyketide synthase (PKS) ACP, determined by two-dimensional ^{1}H-NMR, with the *Escherichia coli* fatty acid synthase (FAS) ACP. The PKS ACP contains four helices (residues 7–16 [A], 42–53 [B], 62–67 [C], 72–86 [D]), and a large loop (residues 17–41) having no defined secondary structure with the exception of a turn between residues 21 and 24. The *act* ACP shows 47% sequence similarity with the *E. coli* FAS ACP and the results demonstrate that the sequence homology is extended to the secondary structure of the proteins.**

Key words: Polyketide; Acyl carrier protein; *Streptomyces*; NMR; Sequential assignment; Secondary structure; Global fold

1. Introduction

The polyketides are a major family of natural products produced mainly by bacteria, fungi and higher plants. They display an enormous variety of structures and biological properties, including pigmentation, antibiosis, immunosuppression and metabolic regulation [1,2]. Despite their structural variety, the polyketides are related by their biosynthetic origin via intermediate 'polyketide chains'. These carbon chains are built by the successive decarboxylative condensation of short-chain carboxylic acids, catalysed by multifunctional enzyme systems, the polyketide synthases (PKSs), which have functional, structural and probably evolutionary relationships with the fatty acid synthases (FASs) [3–5]. Whereas the FAS typically modifies the 2-oxo group after each condensation by a cycle of keto-reduction, dehydration and enoyl reduction to produce a methylene group, this reductive cycle is curtailed or omitted after many or even all condensation steps catalysed by the PKS, leading to the production of carbon chains with a huge variety of functionality. A major challenge in current biosynthetic studies is to achieve an understanding of the factors which control the extent to which this reductive cycle

is employed during each cycle of polyketide chain extension.

The 3D structure of the ACP from the FAS of *E. coli* has been determined at low resolution by NMR methods [6–9]. The *E. coli* FAS ACP exists as a four helix bundle with a hydrophobic core which is presumed to play a role in the stabilisation of growing fatty acid precursors. The structure is conformationally averaged between two or more states [10], perhaps reflecting dynamic properties necessary to accommodate a growing substrate that varies from 2 to 16 carbon atoms during fatty acid biosynthesis. To determine their role in polyketide biosynthesis, the ACPs from the type II PKSs involved in the biosynthesis of the aromatic streptomycete antibiotics actinorhodin (Fig. 1), granaticin, frenolicin and oxytetracycline have been isolated after cloning and expression of the ACP genes in *E. coli* [11]. The present study provides the first structural information on a polyketide synthase component and demonstrates structural homology between the actinorhodin PKS ACP and the FAS ACP from *E. coli*.

2. Materials and methods

2.1. Sample preparation

The *apo*-form of the ACP was isolated as previously described [11]. The protein was dissolved in D_2O (99.90%) or 10% D_2O/90% H_2O to a final concentration of 3–5 mM. Dithiothreitol at equimolar concentrations relative to the protein was included to prevent protein dimerisation via disulphide cross linking involving Cys-17. Measurements were performed in solutions buffered with potassium phosphate (30 mM), pH or p^2H of 4.9 and 5.5.

NMR experiments were performed on a Jeol Alpha 500 MHz spectrometer at 25 or 40°C. Spectra were acquired in phase-sensitive mode with quadrature detection using the method of States et al. [12], with presaturation of the water signal using a DANTE pulse train [13]. The following two-dimensional experiments were run: nuclear Overhauser spectroscopy (NOESY) [14,15] with mixing times of 75, 100, 120 and 150 ms; homonuclear Hartmann-Hahn spectroscopy (HOHAHA) [16] with mixing times of 75 and 100 ms; and double-quantum filtered correlated spectroscopy (DQF-COSY) [17]. The spectral width was set to ±3000 Hz around the residual solvent signal. Data sets were collected with 1024 real points in the t_2 dimension and 256 or 512 t_1 increments. These sets were zero-filled to 2K real points in t_2 and 1000 points in t_1 before Fourier transformation. Amide exchange rates were measured for a series of NOESY spectra recorded over a period of 72 h after dissolving the protein in D_2O. Several spectra were acquired at a proton resonance frequency of 600 MHz on a Varian 600 MHz spectrometer at the Department of Chemistry, University of Edinburgh. DQF-COSY, NOESY with a mixing time of 150 ms and total correlation spectroscopy (TOCSY) [18] spectra with a mixing time of 65 ms were acquired with improved resolution and sensitivity aiding assignments in many cases. $^3J_{NH\alpha}$ coupling constants were extracted from a DQF-COSY data set recorded at 600 MHz and zero filled to 8K complex points in the t_2 dimension.

*Corresponding author. Fax: (44) (117) 9298611.
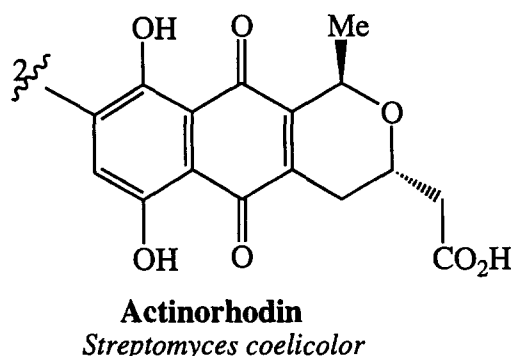E-mail: tom.simpson@bris.ac.uk

Actinorhodin
Streptomyces coelicolor

Fig. 1. Chemical structure of actinorhodin.

3. Results

3.1. Sequential assignment

Unambiguous assignments of spin systems were achieved for 99% of the backbone and side chains using standard two-dimensional assignment techniques [19,20]. Full assignments are listed in Table 1. The majority of the assignments were made using spectra recorded at 25°C and pH 4.9. A few ambiguous cases required the use of a NOESY spectrum recorded at 40°C and spectra at pH 5.5. The 2D NOESY plots indicated high α-helical content from the large number of crosspeaks around the amide diagonal (Fig. 2). Despite the high α-helical content the fingerprint region of the NOESY spectrum was surprisingly well resolved, allowing the assignment to proceed smoothly through the α-helical segments with the majority of CαH-NH(i,i+3) and CαH-NH(i,i+4) contacts resolved at either 25 or 40°C. Characterisation of the helical regions was aided by the measurement of small $^3J_{HN-H\alpha}$ coupling constants (< 6 Hz). Residues 20–41 were difficult to assign due to several degenerate amide protons and the lack of short-range contacts which would have greatly aided sequential assignment. No sequential assignment could be obtained between Arg-34 and Phe-35 due to near amide proton degeneracy at both pH 4.9 and 5.5. The amide resonances of Ile-38 and Gly-39 were degenerate at pH 4.9, but could be resolved sufficiently at pH 5.5 to reveal a weak CαH-NH(i,i+1) nOe. No signals were observed for the N-terminal methionine group which has previously been shown to be post-translationally cleaved during the expression of the *act* ACP in *E. coli*. Ala-2 was assigned from the observation of a single βH-NH(i,i+1) sequential contact to Thr-3. Characteristic CαH-CδH (i−1,i(Pro)) contacts indicated that the two proline residues (Pro-61 and Pro-71), were in the *trans* conformation.

3.2. Secondary structure

The CαH-NH(i,i+3) NOE crosspeaks [21,22] (summarised in Fig. 3) indicate four helical regions for PKS *apo*-ACP from Thr-7 to Glu-16 (**A**), Ser-42 to Gly-53 (**B**), Asp-62 to Arg-67 (**C**), and Arg-72 to Ala-85 (**D**). The presence of CαH-NH(i,i+4) contacts is indicative of α-helix and these sporadically appear throughout these helical regions. It was assumed that their limited observation was sufficient evidence for α-helical secondary structure (rather than 3_{10} helix). Helices B and C are separated by a short stretch of extended peptide

chain (54–61) whilst helices C and D are connected by a tight turn involving residues 67–70. The sequence from Thr-3–Thr-7 is characterised by strong CαH-NH(i,i+1) contacts with no NH-NH(i,i+1) nOes observed, indicating an extended structure at the N-terminus of the protein.

The structure adopted by the polypeptide between helices A and B (residues 17–42) is more difficult to define using short range contacts alone as it does not appear to conform to an overall common motif. A sequential turn appears between residues 21–24 on the evidence of strong CαH-NH(i,i+2), CβH-NH(i,i+2) and CαH-NH(i,i+1) contacts. Slow amide exchange was not observed, however, for any of the residues 21–24 which are probably solvent exposed. Residues 18–25 contain several hydrophilic residues (Glu-20, Asp-22, Asp-25) having no observable long-range contacts, and negligible amide exchange protection indicating this region is solvent exposed and probably highly flexible. The remaining segment of the loop between helices A and B is more structured, containing many hydrophobic residues with numerous short range inter-side chain nOes and several long-range nOes. Residues Leu-33, Arg-34 and Ile-38 are highly exchange protected indicating that this region may be buried and part of the core of the protein.

The observation of slowly exchanging amide protons is characteristic of stable secondary structure [23]. Amide resonances persisting after 4 h at pH 4.9 (exchange protection factors of at least 100-fold [24]) were considered to be hydrogen-bonded within stable elements of secondary structure. Slowly exchanging amide protons were observed for residues Leu-10 to Val-15, Ala-49 to Glu-53 and Glu-73 to Gly-80. Apart from Glu-73 NH, the amides appear in regions of assigned α-helix and are involved in helical hydrogen bonding. Glu-73 is present at the beginning of the fourth helix and cannot participate in an α-helical hydrogen bond. This amide may be hydrogen bonded within the tight turn between helix C and D. The short helix C consisting of only 6 residues (62–67) has low stability with amide exchange protection factors less than 100-fold.
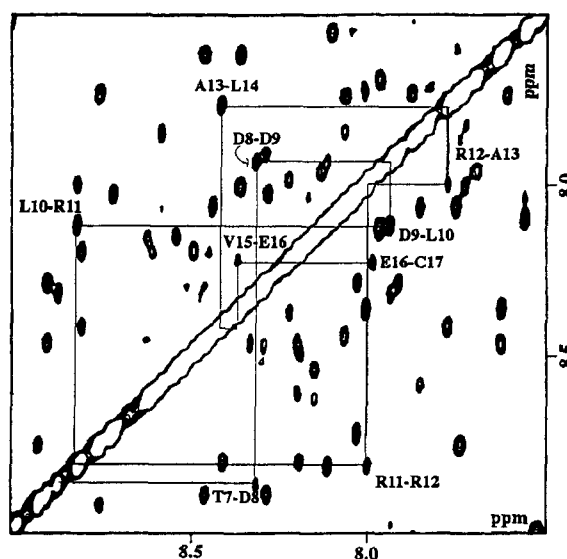

Fig. 2. Amide diagonal region of a 150 ms NOESY spectrum of actinorhodin *apo*-ACP at 25°C, pH 4.9 in 90%/10% H_2O/D_2O showing the crosspeaks for helix A. Only positive contours are plotted.

Table 1
Sequential resonance assignzments for *apo*-ACT ACP

Residue	Chemical shifts				
	NH	$C^\alpha H$	$C^\beta H/C^{\beta'} H$	$C^\gamma H/C^{\gamma'} H$	Others
Ala-2	8.05	4.31	1.52		
Thr-3	8.72	4.44	4.22	1.42	
Leu-4	8.19	4.38	1.60,1.48	1.711	$C^\delta H_3$ 0.90,0.97
Leu-5	9.47	4.54	1.34,1.34[a]	1.59	$C^\delta H_3$ 0.70,0.68
Thr-6	9.00	4.80	4.87	1.42	
Thr-7	8.88	3.88	4.37	1.40	
Asp-8	8.33	4.64	2.73,2.73[a]		
Asp-9	7.94	4.58	2.75,3.12		
Leu-10	8.13	4.22	1.44,1.88	1.18	1.15,1.04
Arg-11	8.83	3.57	2.02,2.08	1.18,1.43	$C^\delta H_2$ 3.16,3.23 $N^\epsilon H$ 7.33
Arg-12	8.01	4.05	2.03,1.93	1.71,1.71[a]	$C^\delta H_2$ 3.33,3.40 $N^\epsilon H$ 7.56
Ala-13	7.75	4.42	1.70		
Leu-14	8.45	4.34	1.44,1.99	1.90	0.93,0.77
Val-15	8.37	3.91	2.26		$C\gamma H_3$ 1.14, 1.05
Glu-16	8.24	4.23	2.35,2.35[a]	2.68,2.47	
Cys-17	8.02	4.50	3.13,3.07		
Ala-18	7.92	4.38	1.59		
Gly-19	8.30	4.06,4.13			
Glu-20	8.47	4.06	2.05,2.21	2.42,2.42[a]	
Thr-21	8.30	4.54	4.40	1.25	
Asp-22	8.54	4.76	2.90,2.90[a]		
Gly-23	8.56	4.30,4.30[a]			
Thr-24	8.16	4.33	4.26	1.30	
Asp-25	8.64	4.73	2.94,2.80		
Leu-26	8.45	4.36	1.48,1.23	1.60	$C^\delta H_3$ 0.73,0.84
Ser-27	8.19	4.29	4.07,4.01		
Gly-28	8.62	4.26,3.92			
Asp-29	8.73	4.92	2.93,2.72		
Phe-30	8.12	4.77	3.05,3.33		$C^\delta H$ 7.26 $C^\epsilon H$ 7.26 $C^\zeta H$ 7.23
Leu-31	7.52	3.31	1.05,1.64	1.24	$C^\delta H_3$ 0.81,0.49
Asp-32	8.05	5.08	3.07,2.39		
Leu-33	7.24	4.32	1.78,1.40	1.42	$C^\delta H_3$ 0.98,1.08
Arg-34	8.48	4.78	1.97,1.67	2.20,2.20[a]	$C^\delta H_2$3.47,3.37 $N^\epsilon H$ 7.93
Phe-35	8.54	4.40	3.61,3.12		$C^\delta H$ 7.13 $C^\epsilon H$ 6.96 $C^\zeta H$ 6.93
Glu-36	9.59	4.38	2.17,2.26	2.59,2.59[a]	
Asp-37	7.62	4.66	3.12,3.04		
Ile-38	7.74	4.66	2.44		$C^\gamma H$ 1.84,1.54 $C^\gamma H_3$ 1.07 $C^\delta H_3$ 0.91
Gly-39	7.76	4.30,3.90			
Tyr-40	8.07	4.64	3.02,2.85		$C^\delta H$ 6.77 $C^\epsilon H$ 7.00
Asp-41	8.08	4.77	3.21,2.83		
Ser-42	8.60	4.21	4.01,4.07		
Leu-43	7.84	4.26	1.88,1.78	1.73	$C^\delta H_3$1.01,1.07
Ala-44	8.07	4.33	1.59		
Leu-45	8.47	3.86	1.69,1.48	1.34	$C^\delta H_3$0.38,0.28
Met-46	8.32	4.26	2.37,2.25	2.89,2.76	
Glu-47	8.35	4.27	2.76,2.38	2.76,2.90	
Thr-48	8.42	4.26	4.37	1.53	
Ala-49	8.83	3.97	1.55		
Ala-50	8.20	4.27	1.65		
Arg-51	8.20	4.28	2.23,2.11	1.94,1.80	$C^\delta H_2$3.30,3.39 $N^\epsilon H$7.63
Leu-52	8.50	4.31	2.05,2.20		0.89,1.06
Glu-53	9.08	4.07	2.28,2.20	2.58,2.35	
Ser-54	8.04	4.42	4.12,4.12[a]		
Arg-55	8.08	4.28	1.70,1.93	1.36,1.02	$C^\delta H_2$ 3.07,3.07 $N^\epsilon H$ 7.22
Tyr-56	8.14	4.70	3.50,2.79		$C^\delta H$ 7.47 $C^\epsilon H$ 6.83
Gly-57	7.96	4.11,4.11[a]			
Val-58	7.70	4.76	2.13		$C\gamma H_3$ 0.93,0.98
Ser-59	8.53	4.78	3.82,3.76		
Ile-60	8.01	4.68	1.91	1.44,1.10	$C^\gamma H_3$1.054 $C^\delta H_3$ 0.85
Pro-61		4.49	2.53,2.53	2.02,2.02[a]	
Asp-62	8.94	4.45	2.28,2.78		
Asp-63	8.77	4.48	2.80,2.80[a]		
Val-64	7.40	3.82	2.24		$C\gamma H_3$ 1.10,1.03
Ala-65	8.18	3.98	1.42		
Gly-66	8.05	4.13,3.93			
Arg-67	7.45	4.68	1.80,1.90	2.10,2.10	$C^\delta H$ 3.31,3.31 $N^\epsilon H$ 7.37
Val-68	7.31	4.39	2.46		$C^\gamma H_3$ 1.27,1.18

Table 1 (continued)

Residue	Chemical shifts				
	NH	$C^{\alpha}H$	$C^{\beta}H/C^{\beta'}H$	$C^{\gamma}H/C^{\gamma}H$	Others
Asp-69	9.04	5.28	3.07,2.93		
Thr-70	7.52	5.05	4.69	1.10	
Pro-71		3.59	2.15,2.57	2.30,2.37	2.75, 3.96
Arg-72	9.06	3.65	1.90,1.68	1.62,1.54	$C^{\delta}H$ 3.02,3.57 $N^{\varepsilon}H$ 9.08
Glu-73	7.88	4.25	2.24,2.46	2.52,2.62	
Leu-74	7.72	4.32	2.44,1.72	0.99	$C^{\delta}H_3$ 1.07,1.17
Leu-75	8.76	3.90	1.58,2.20	1.71	$C^{\delta}H_3$ 0.90,0.82
Asp-76	8.71	4.50	2.78,2.82		
Leu-77	8.03	4.30	2.05,1.87	0.87	$C^{\delta}H_3$ 0.97,0.97[a]
Ile-78	8.29	3.75	1.939	1.29,1.74	$C^{\gamma}H_3$ 0.87 $C^{\delta}H_3$ 0.82
Asn-79	8.90	4.92	3.12,2.78		$^{\gamma}NH_2$ 7.34,7.69
Gly-80	8.47	4.05,4.53			
Ala-81	7.63	4.45	1.65		
Leu-82	8.37	4.20	2.04,2.04[a]	1.58	$C^{\delta}H_3$1.00,1.00
Ala-83	7.98	4.27	1.63		
Glu-84	7.73	4.41	2.17,2.30	2.55,2.62	
Ala-85	7.83	4.50	1.62		
Ala-86	8.01	4.25	1.57		

^{1}H chemical shifts (± 0.01) are expressed in ppm for ACT ACP at pH 4.9, 25°C. Internal reference H_2O, 25°C.
[a]The degeneracy of the $C^{(\beta,\gamma,\delta)}H$ protons is inferred.

4. Discussion

The sequential assignment of the NMR spectrum of the actinorhodin PKS ACP has resulted in near complete assignments for all residues. The secondary structure of the PKS ACP is predominantly α-helix (49%), four regions being identified (7–16 [A]; 42–53 [B]; 62–67 [C]; 72–85 [D]). Helices A and B are separated by a loop (residues 17–41) which is poorly defined over residues 18–25 although a tight turn has been identified between Thr-21 and Thr-24. The latter part of the loop, between 26 and 42 shows many more short range inter-side chain contacts and long-range nOes suggesting this region is well buried and more highly structured.

Comparing the E. coli fatty acid synthase (FAS) ACP with the S. coelicolor polyketide ACP, a common overall secondary structure of four helices is apparent. The FAS ACP is a soluble, cytosolic protein (77 amino acids, 8847 Da) which carries a fatty acid via a thioester linkage to a phosphopantetheine prosthetic group. This prosthetic group is covalently attached to a serine residue (Ser-36) located within a highly conserved amino acid region. This region is common to all ACPs. The FAS ACP is highly α-helical (slightly higher overall than the PKS ACP at 60% α-helical secondary elements) and like the polyketide ACP is based around a four helix motif (H1: 3–15; H2: 37–51; H3: 56–63; H4: 65–75). The structure is dominated by helices 1, 2 and 4, with 2 and 4 approximately parallel to each other, and anti-parallel at an angle of 150° to helix 1. The four helices are linked by a series
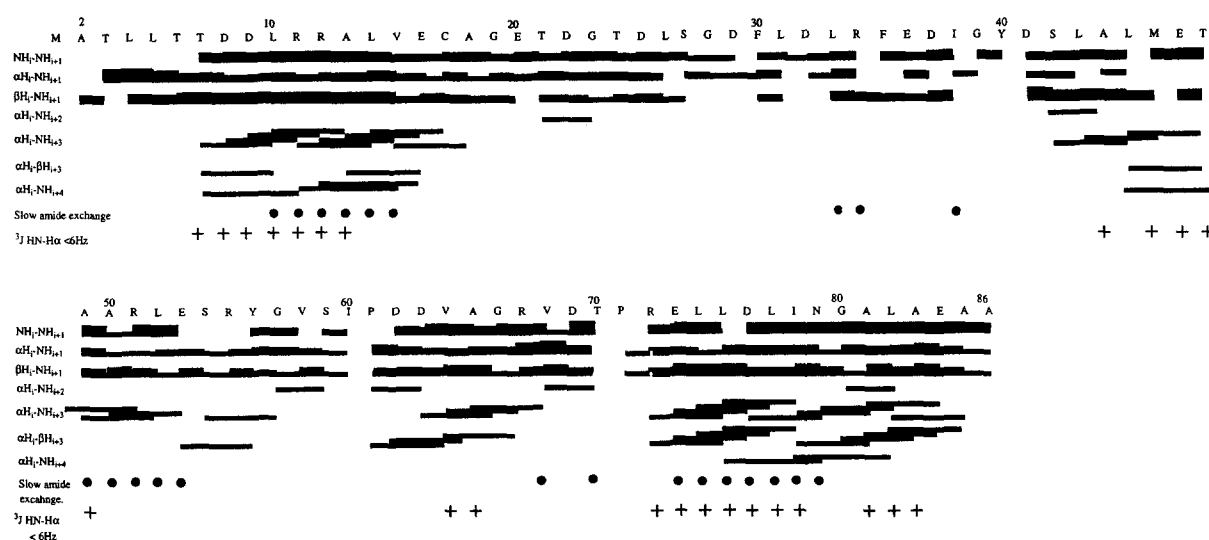

Fig. 3. Amino acid sequence of actinorhodin apo-ACP with a summary of all short-range NOE correlations involving the NH, Cα and Cβ protons. The thickness of the bars is an approximate guide to the observed NOE intensity in the 150 ms NOESY experiment in 90%/10% H_2O/ D_2O, 25°C and pH 4.9. A dashed bar indicates an nOe that was uncertain due to overlap of resonances and a blank space indicates a position where no NOE was detected. Slowly exchanging amides are indicated by a filled circle, while measured coupling constants < 6 Hz are shown by the symbol '+'.

Granaticin ACP *Streptomyces violaceoruber*		EELGYDSLAL[44]
Actinorhodin ACP *Streptomyces coelicolor*		EDIGYDSLAL[45]
Griseusin ACP *Streptomyces griseus*		EELGYESLAL[46]
Oxytetracycline ACP *Streptomyces rimosus*		DALGYDSLAL[44]
Fatty Acid ACP *E. coli*		EDLGADSLDT[39]

Fig. 4. Comparison of the amino acid sequences surrounding the cofactor binding serine residue of four streptomycete polyketide synthase ACPs and *E. coli* fatty acid synthase ACP. The highly conserved D-S-L motif is highlighted for the proteins.

of loops, the local structures of which are less well defined than those of the helical elements and similar therefore to regions connecting the helices in the PKS ACP.

The positions of the four helices are conserved between the two proteins, though with the exception of helix D, they are slightly shorter in the PKS ACP. Helix D is the longest α-helix in this ACP and is the most stable judging by the exchange stability of its amide protons. In the FAS ACP NH-NH(i,i+1)) nOes are observed starting at residue 3 [10] whereas in the PKS ACP the N-terminus is extended up to residue 7. The N-terminus of helix B is highly conserved with respect to positioning and sequence homology with the helix II of FAS ACP (Fig. 4). In PKS and FAS ACP Ser-42 and Ser-36 form the N-terminus of the second helix, respectively. Thus, the highly conserved D-S-L sequence, common to almost all PKS and FAS ACPs, also appears to be positioned in a conserved segment of secondary structure. Indeed, the ACPs from several type II PKSs accumulate a significant amount of the *holo* form when expressed in *E. coli* [11]. This modification relies on recognition of the heterologous ACP by the *E. coli holo*-ACP synthase and indicates that the carrier protein can act as a substrate for this *E. coli* enzyme. The observed conservation of secondary structure around the serine provides structural evidence to support the observed functional behaviour.

In the *E. coli* structure, all four helices are amphipathic. Hydrophobic residues on the three main helices define a hydrophobic cavity. NMR studies [6] on acylated FAS ACP indicate that the saturated chain is held in this cavity. A growing polyketide chain retains a higher oxidation state during biosynthesis than the equivalent fatty acid, however, and the cleft of the ACP is expected to be less hydrophobic to accommodate an inherently unstable, highly functionalised molecule. A suitable arrangement of potential hydrogen bonding sites may form a stabilising environment for different parts of the growing polar polyketide chain. The NMR chemical shifts of the δC protons of Arg-72 are split by 0.55 ppm in the PKS ACP suggesting that this residue is immobilised or partially buried. Similar splitting of the δC protons for Arg-71 (*otc*) and Arg-73 (*gris*) is observed in the oxytetracycline and griseusin ACPs (unpublished results). This arginine residue is conserved within all the polyketide ACPs and may have a role in providing a more polar environment within the core of the protein, although at present no direct evidence for an association between the growing polyketide chain, and amino acids within the protein core is available.

In conclusion our findings suggest that a strong secondary structure homology exists between FAS ACP and PKS ACP and it may be speculated that this extends to the three-dimensional structure as well. Recent evidence supports this where actinorhodin PKS ACP was genetically replaced by alterna-

tive polyketide synthase ACPs and even a fatty acid synthase ACP to produce an apparently functional PKS [25,26]. However, quantitative and possibly qualitative differences in the pigments produced by the genetically manipulated organisms in these experiments suggest that some important differences between the polyketide ACPs and fatty acid ACPs cannot be precluded. The tertiary structure of the actinorhodin PKS ACP is currently being determined. This will allow direct structural comparisons between polyketide ACPs as well as with the FAS ACP from *E. coli*.

References

[1] O'Hagan, D. (1991) The Polyketide Metabolites, Ellis Horwood, Chichester.
[2] Simpson, T.J. (1991) Nat. Prod. Rep. 8, 573-602.
[3] Hopwood, D.A. and Sherman, D.H. (1990) Annu. Rev. Genet. 24, 37-66.
[4] Robinson, J. (1991) Phil. Trans. R. Soc. Lond. B. 332, 107-114.
[5] Hopwood, D.A. and Khosla, C. (1992) Foundation Symposium No. 171, Wiley, Chichester, pp. 88-112.
[6] Mayo, K.H. and Prestegard, J.H. (1985) Biochemistry 24, 7834-7838.
[7] Holak, T.A., Nilges, M., Gronenborn, A.M., Clore, G.M. and Prestegard, J.H. (1988) Eur. J. Biochem. 175, 9-15.
[8] Holak, T.A., Kearsley, J.K., Kim, Y. and Prestegard, J.H. (1988) Biochemistry 27, 6135-6142.
[9] Kim, Y. and Prestegard, J.H. (1990) Proteins: Struct. Funct. Genet. 8, 377-385.
[10] Kim, Y. and Prestegard, J.H. (1989) Biochemistry 28, 8792-8797.
[11] Crosby, J., Sherman, D.H., Bibb, M.J., Revill, W.P., Hopwood, D.A. and Simpson, T.J. (1995) Biochim. Biophys. Acta 1251, 32-42.
[12] States, D.J., Haberkorn, R.A. and Ruben, D.J. (1982) J. Magn. Reson. 48, 286-292.
[13] Morris, G.A. and Freeman, R. (1978) J. Magn. Reson. 29, 433-462.
[14] Jeener, J., Meier, B.H., Bachman, P. and Ernst, R.R. (1979) J. Chem. Phys. 71, 4546-4553.
[15] Wider, G., Macura, S., Kumar, A., Ernst, R.R. and Wüthrich, K. (1984) J. Magn. Reson. 56, 207-234.
[16] Rance, M. (1987) J. Magn. Reson. 74, 557-564.
[17] Rance, M., Sorenson, O.W., Bodenhausen, G., Wagner, G., Ernst, R.R. and Wüthrich, K. (1983) Biochim. Biophys. Commun. 117, 479-485.
[18] Braunschweiler, L. and Ernst, R.R. (1983) J. Magn. Reson. 53, 521-528.
[19] Wüthrich, K. (1986) NMR of Proteins and Nucleic Acids, Wiley, New York.
[20] Wagner, G. and Wüthrich, K. (1982) J. Mol. Biol. 155, 347-366.
[21] Wüthrich, K., Billeter, M. and Braun, W. (1984) J. Mol. Biol. 180, 715-740.
[22] Williamson, M.P., Marion, D. and Wuthrich, K. (1984) J. Mol. Biol. 173, 341-359.
[23] Wagner, G. and Wüthrich, K. (1982) J. Mol. Biol. 160, 343-361.
[24] Bai, Y. Milne, S.S., Mayne, L. and Englander, S.W. (1993) Proteins Struct. Funct. Genet. 17, 75-86.
[25] Khosla, C., Ebert-Khosla, S., Torres, R. and Hopwood, D.A. (1992) Mol. Microbiol. 6, 3237-3249.
[26] Khosla, C., McDaniel, R., Ebert-Khosla, S., Torres, R., Sherman, D.H., Bibb, M.J. and Hopwood, D.A. (1993) J. Bacteriol. 175, 2197-2204.